CONF-9104174--1

DE91 009931

EVALUATION OF FILLER METALS FOR HIGH-STRENGTH STAINLESS STEELS

R. W. Swindeman, G. M. Goodwin, and J. F. King
Oak Ridge National Laboratory
Oak Ridge, Tennessee 37831

and

C. D. Lundin and C. Y. P. Qiao
University of Tennessee
Knoxville, Tennessee 37916

"The submitted manuscript has been authored by a contractor of the U.S. Government under contract No. DE-AC05-84OR21400. Accordingly, the U.S. Government retains a nonexclusive, royalty-free license to publish or reproduce the published form of this contribution, or allow others to do so, for U.S. Government purposes."

EVALUATION OF FILLER METALS FOR HIGH-STRENGTH STAINLESS STEELS

ABSTRACT

Weldments were produced in types 316, 17-14CuMo, and high strength 14Cr-16Ni-2Mo stainless steel base metals with four filler metals- alloy 82, 17-14CuMo stainless steel, "controlled residual element" CRE 16-8-2 stainless steel, and alloy 556. The welds were evaluated on the basis of microstructure, strength, and ductility. All of the base metals were prone to hot cracking, but steels high in phosphorus were the most likely to produce poor welds. The CRE 16-8-2 stainless steel filler metal produced the best combination of creep strength and ductility, while alloy 556 produced the best long-time creep strength. Tensile and creep failures usually occurred in the alloy 82, 17-14CuMo stainless steel, or CRE 16-8-2 stainless steel filler metal of weldments tested transverse to the weld. At low temperatures (600 to 700°C) and short times the alloy 556 filler metal usually failed, while at high temperature (700 to 800°C) and long times, the weldment usually failed in the base metal. In weldments creep tested parallel to the welding direction cracking initiated in the CRE 16-8-2 stainless steel filler, even though cracks were observed in the heat-affected zone of the base metal. The mechnaical performance of weldments in 14Cr-16Ni-2Mo stainless steel tubing alloys was satisfactory in spite of the observed tendency for cracking. However, it was concluded that further development of the welding technology would be needed before the high-strength alloys would be commercially acceptable.

EVALUATION OF FILLER METALS FOR
HIGH-STRENGTH STAINLESS STEELS

INTRODUCTION

Exceptional creep strength and metallurgical stability have been produced in modified type 316 stainless steels that contain nitrogen and MC-type carbide-forming elements such as niobium, titanium, and vanadium (1,2,3). With optimized thermal-mechanical processing, more than twice the creep strength of type 316 stainless steel may be achieved at temperatures in the range 650 to 750°C, and good metallurgical stability has been demonstrated for testing times to 50,000 h. Because of low cost and ease of fabrication, the lean stainless steel alloys have several potential applications in the fossil and nuclear power industries. In advanced steam cycle applications, the higher strength allows thinner tube walls, thus reducing fireside temperatures and thermal stresses. Due to low chromium content, however, it seems likely that cladding would be required in many applications above 600°C. Further, the compositional adjustments that promote strength and ductility of base metal suppress ferrite formation during solidification resulting in a potential for cracking problems in weldments (4,5). To allow service in pressure envelopment applications, the extent of the hot cracking and liquation cracking in the heat affected zone must be assessed, and their influences on the structural integrity of weldments must be determined. The severity of cracking may be reduced by the selection of a filler metal of a different composition may be an option. This paper provides an overview of some of the examinations being undertaken to evaluate filler metals for a group of lean stainless steels developed under sponsorship of the U.S. Department of Energy (6).

MATERIALS

Base metals included type 316 stainless steel, 17-14CuMo stainless steel, and developmental 14Cr-16Ni-2Mo stainless steels containing various combinations of the MC-type carbide-forming elements such as titanium, vanadium, and niobium. The developmental alloys were grouped under the generic identification "HT-UPS" ("high temperature, ultrafine precipitate strengthened") (7). The product forms and chemistries for the alloys are provided in Table 1. Most of the research was performed on plate products, but some examinations were performed on bare and clad tubing. Cladding materials were alloys 671 and 690 which were powder products co-extruded at 1200°C (8). In regard to chemistries, the HT-UPS alloys had low chromium equivalencies. Chromium and nickel equivalencies calculated from the DeLong equations (9) revealed that type 316 stainless steel had the highest chromium equivalency, type 17-14CuMo stainless steel was next, and the HT-UPS alloys were balanced on the nickel side. High nickel equivalencies caused welding problems. Also important in the investigation of weldability was the phosphorus content, which ranged from less than 0.03% to more than 0.07% in the HT-UPS alloys. Filler metals used for joining the base metals included alloy 82, 17-14CuMo stainless steel, CRE 16-8-2 stainless steel, and alloy 556. The controlled residual elements in the CRE 16-8-2 stainless steel were titanium, phosphorus, and boron. Alloy 92, and alloy 72 were used for weld overlay cladding and no problems were encountered with the low phosphorus alloys.

CHARACTERIZATION OF THE CRACKING TENDENCY

The investigation of the hot cracking susceptibility of base metals included Sigmajig, Varestraint, and Gleeble testing (4,10). The Sigmajig testing ranked type 316 stainless steel as the least prone to hot cracking, type 17-14CuMo stainless steel as marginal, and the developmental HT-UPS alloys as likely to produce hot cracks. Comparative data produced in the Sigmajig are provided in Fig. 1. The data obtained in the Varestraint tests ranked type 316 stainless steel better than the HT-UPS alloys, and typical trends have been plotted in Fig. 2. Finally, the Gleeble testing confirmed trends shown by the two other hot cracking evaluations (4). The data strongly suggested that autogenous welding of the 17-14CuMo stainless steel would be marginal, and the HT-UPS alloys would require a dissimilar filler metal.

PRODUCTION OF WELDMENTS

The 13-mm-thick plates were welded under full restraint obtained by fillet welding the plates to a 25-mm-thick type 316 stainless steel backing plate. A V-weld configuration was used and the root pass was approximately 6 mm wide, which allowed some dilution from the base metal of the backing plate. Tubing was restrained by fillet welding plates to the tubing. These plates were locked into a sturdy jig illustrated in Fig. 3. Typically, the root pass in the tubing was 4 to 5 mm wide. Bare tubing was butt welded in several conditions: cold pilgered and annealed, hot extruded, hot extruded plus 5, 10, and 12% cold sinking, and after a creep exposure for 2500 h at 700°C and 140 MPa. Tubing clad with alloy 671 was butt welded in the as-extruded condition. Simulated longitudinal and transverse partial-penetration repair welds were introduced into the clad tubing.

Not all filler metals were used on all alloys, and a listing of the combinations that were examined is provided in Table 2. Gas tungsten arc (GTA) welds were produced in type 316 stainless steel plate using the CRE 16-8-2 stainless steel filler metal, while both GTA and shielded metal arc (SMA) welds were produced in the type 17-14CuMo stainless steel plate. The HT-UPS plates were welded with four filler metals: alloy 82 (GTA), type 17-14CuMo stainless steel (SMA), CRE 16-8-2 stainless steel (GTA), and alloy 556 (GTA). On the clad tubing, the base metal was welded with CRE 16-8-2 (GTA) and the overlay cladding with alloy 82 (GTA).

EXAMINATION OF WELDMENTS

Transverse specimens of the welds were evaluated by metallography, side bend tests, and in some cases hardness traverses. Evidence of cracking was found in all of the high phosphorus alloys and most of the HT-UPS alloys. Often, the cracking was too minute to be detected in the side bend test. When it was observed, cracks were usually emanating from the fusion line and into the heat-affected zone (HAZ) of the base metal. However, the extent of cracking varied with the specific alloy, the degree of restraint, and the filler metal. A typical photomicrograph of a weldment in a high phosphorus alloy (AX7) that severely cracked is shown in Fig. 4. Here, the filler metal was type 17-14CuMo stainless steel. A photomicrograph is shown in Fig. 5 of a weldment in a low phosphorus alloy (BWT4) that was less prone to cracking. Hot cracks and liquation in the HAZ were often observed in the HT-UPS alloys, but penetration of some filler metals along grain boundaries open to the fusion zone minimized cracking. Generally, grain coarsened regions were found in the type 316 stainless steels and the fine grained HT-UPS alloys. The coarser grained HT-UPS alloys exhibited little evidence of grain growth but some regions of grain boundary migration. A typical hardness traverse is shown in Fig. 6 for welded tubing. Here, the filler metal was CRE 16-8-2 stainless steel and the tubing was a HT-UPS alloy (BWT4) in the hot extruded condition. Superimposed on the original hardness profile is one that was obtained after 2500 h at 700 °C. In both cases the weld metal and HAZ regions exhibited similar hardness values.

MECHANICAL BEHAVIOR

Tensile and creep tests were performed on weldments, and sketches of the specimen configurations are provided in Fig. 7. Most testing was performed on bar specimens which were oriented perpendicular to the welding direction (transverse specimens), so as to include filler metal, HAZ, and base metal in the test section. However, a few tests were performed on all weld metal specimens machined in the longitudinal direction of welds of type 316 stainless steel/CRE 16-8-2 stainless steel weldments. Two full scale tubes (64-mm-diam.) were tested. Two longitudinal tests were performed on plates of type 316 stainless steel/CRE 16-8-2 stainless steel and two on HT-UPS/CRE 16-8-2 stainless steel.

Tensile test data were collected at room temperature and 700°C on weldments of more than 20 combinations of base metals and filler metals. The information of primary interest was in the failure location and ductility based on reduction of area (RA). Failures were observed in base metal, HAZ, fusion line, and weld metal. In most weldments the RA values exceeded 40%, regardless of the failure location. The exceptions were the combinations of high phosphorus heats welded with 17-14CuMo stainless steel filler metal. Here, values in the range 15% to 30% were observed.

Approximately 80 stress-rupture tests were performed on weldments of different combinations of base metals and filler metals. For the HT-UPS alloys the temperatures were in the range 600 to 800°C and times ranged from 10 to beyond 10,000 h. Test data were available for the combination of type 316 stainless steel base metal and CRE 16-8-2 filler metal at temperatures in the range 538 to 650°C. The information of primary interest included the strength relative to base metal, the failure location, and the failure ductility determined by the reduction of area (RA). To cover the broadest range of variables the test data were compared on the basis of log stress versus the Larson-Miller parameter (LMP) for rupture life. The parametric constant was chosen to be 20, commonly used for austenitic stainless steels.

In Fig. 8, rupture data for three base metals have been plotted. These include type 316 stainless steel (Fig. 8a) (11), 17-14CuMo stainless steel (Fig. 8b) (6), and the HT-

UPS alloys (Fig. 8c) (6). Trend curves were drawn through each data set for purposes of comparison with weldment data. In Fig. 9 weldment data have been plotted and compared with the base metal trends. Here, it may be seen that at low values of the LMP weldments made with the CRE 16-8-2 stainless steel filler metal were comparable in strength to type 316 stainless steel, but with increasing LMP the strength approached that for 17-14CuMo stainless steel. For long times or higher temperatures (large LMP values) weldments with alloy 556 filler metal were the strongest and were comparable to the strength of the HT-UPS base metal.

In Fig. 10 the RA data for weldments have been plotted against the log of the rupture life. Included are data for three filler metals CRE 16-8-2, 17-14CuMo stainless steel, and alloy 556. Generally, the CRE 16-8-2 filler metal produced the best ductility, while the 17-14CuMo stainless steel filler metal was brittle. The RA data values for alloy 82 were good, but only two weldments were tested. The RA values for alloy 556 were high at short times but tended to diminish with increasing LMP. Testing to high values of the LMP are in progress for the alloy 556 filler metal.

The tests of weldments oriented with the weld parallel to the stress direction (longitudinal specimens) were of considerable interest because they provided a means of investigating the strain tolerance of different regions of the weldment under creep conditions. These specimens had equal areas of base metal and weld metal, and the surfaces of the specimens were observed through a window in the furnace during the creep testing An interesting contrast was found in comparing the cracking patterns for the weldments of type 316 stainless steel and the HT-UPS alloy when both were welded with CRE 16-8-2 filler metal and tested at 650°C. Photomicrographs showing this contrast are provided in Fig. 11. Cracking in the type 316 stainless steel weldment initiated in the coarse-grained HAZ near the fusion line and cracks propagated into both base metal and weld metal (Fig. 11a). Cracking in the HT-UPS alloy initiated in the CRE 16-8-2 weld metal and propagated toward the fusion line. When all of the weld metal was cracked the remaining stress in the HT-UPS ligaments exceeded the ultimate tensile strength of the material and a ductile overload failure occurred. No hot crack growth was observed in the longitudinal welds of the HT-UPS alloy.

CONCLUSIONS

The performance of weldments in austenitic boiler tubing and main steam lines is of great concern. Factors such as reducing chromium, adding nitrogen, and MC forming elements which improve creep rupture strength tend to cause weld cracking problems. The severity of the problem may be mitigated by the judicious selection of filler metal. Data accumulated in this research effort suggest that 17-14CuMo stainless steel filler metal would be a poor choice because stress rupture ductilities were too low. In contrast, the CRE 16-8-2 stainless steel filler metal produced a weldment with good ductility and strength at longer times. As an alternative for temperatures exceeding 650°C, alloy 556 shows some potential. However, longer time testing is required before this alloy can be considered as a substitute for filler metals such as alloy 82.

ACKNOWLEDGEMENTS

This research was sponsored by the U.S. Department of Energy, Fossil Energy Advanced Research and Technology Development (AR&TD) Materials Program, COE/FE AA 15 10 10 0, Work Breakdown Structure Element ORNL-2(B), DE-AC05-84OR21400 with Martin Marietta Energy Systems, Inc.. Much of the testing was performed by E. Bolling. The paper was reviewed by M. J. Santella, D. J. Alexander, and R.R. Judkins.

REFERENCES

1. E. C. Chapman and R. E. Lorentz, Jr., "The Selection of Materials and Fabricating Techniques for the Eddystone Boiler and Sulzer Control Valves," Journal of Engineering for Power, Trans. American Society of Mechanical Engineers, 1960, p. 275.

2. Y. Sawaragi and S. Hirano, "The Development of a New 18-8 Austenitic Steel (0.1C-18Cr-9Ni-3Cu-Nb,N) with High Elevated Strength for Fossil Fired Boilers," in New Alloys for Pressure Vessels and Piping, PVP-Vol. 201, American Society of Mechanical Engineers, New York, NY, 1990, p. 141.

3. Y. Minami, H. Kimura, and M. Tanimura, "Creep Rupture Properties of 18%Cr-8%Ni-Ti-Nb and Type 347H Austenitic Stainless Steels," in New Developments in Stainless Steel Technology, American Society for Metals, Metals Park, OH, 1985, p. 231.

4. V. P. Kujanpää, S. A. David, and C. L. White, "Characterization of Heat-Affected Zone Cracking in Austenitic Stainless Steel Welds," Welding Research Supplement, August, 1987, p. 221s.

5. C. D. Lundin, et al., "HAZ Liquation Cracking Behavior in Newly Developed Lean 316 Stainless Steel," in New Alloys for Pressure Vessels and Piping, PVP-Vol.201, American Society of Mechanical Engineers, New York, NY, 1990, p. 155.

6. R. W. Swindeman, et al., Evaluation of Advanced Austenitic Alloys Relative to Alloy Design Criteria for Steam Service, Part 1- Lean Stainless Steels, ORNL-6629/P1, Oak Ridge National Laboratory, May, 1990.

7. P. J. Mazaisz, "Developing an Austenitic Stainless Steel for Improved Performance in Fossil Power Facilities," Journal of Metals, Vol. 41, 1989, p. 14.

8. S. E. LeBeau, Production of Small Heats of Austenitic Tubing- Final Report CRD#1191, Babcock & Wilcox report RDD;89:4423-01-01:01, Alliance, OH, 1988.

9. W. T. DeLong, "Ferrite in Austenitic Stainless Steel Weld Metal," Welding Journal, pp. 273-s , 1974.

10. G. M. Goodwin, "Development of a New Hot-Cracking Test- The Sigmajig," Welding Journal (Miami), Vol. 66, pp. 33s, 1987.

11. National Research Institute for Metals, Data Sheets on the Elevated-Temperature Properties of 18Cr-12Ni-Mo Stainless Steel Bars for General Application (SUS 316-B)," Data Sheet No. 15A, NRIM, Tokyo, Japan, 1982.

Table 1. Chemistry for Base and Filler Metals

Alloy	Product	C	Si	Mn	Fe	Ni	Cr	Ti	Nb+Ta	V	Mo	P	B	S	N	Cu	Other
316 SS	Plate, Tubing	0.057	0.58	1.86	bal	13.50	17.2	0.02			2.34	0.024		0.019	0.030	0.10	
17-14CuMo SS	Forging	0.098	0.95	0.83	bal	13.80	16.5	0.21	0.45	0.07	1.96	0.014		0.005	0.025	3.34	
HT-UTS CE0	Plate	0.072	0.41	1.80	bal	16.00	14.2	0.24	0.10	0.57	2.45	0.071	0.005	0.007	0.015		
HT-UTS CE1	Plate	0.085	0.21	1.64	bal	16.20	13.1	0.21	0.12	0.52	2.30	0.076	0.005	0.008	0.016	0.04	
HT-UTS CE2	Plate	0.079	0.26	1.89	bal	16.00	16.1	0.31	0.11	0.58	2.26	0.069	0.007	0.008	0.017		
HT-UTS CE3	Plate	0.086	0.21	1.75	bal	16.20	14.5	0.27	0.12	0.56	2.41	0.071	0.005	0.008	0.012	1.96	
HT-UTS AX5	Plate	0.076	0.12	2.04	bal	16.20	13.9	0.27	0.15	0.52	2.46	0.024	0.005	0.015	0.021		
HT-UTS AX6	Plate	0.074	0.12	1.96	bal	16.00	14.3	0.28	0.15	0.51	2.48	0.041	0.005	0.015	0.020		
HT-UTS AX7	Plate	0.073	0.11	2.00	bal	16.00	14.2	0.18	0.15	0.53	2.48	0.073	0.005	0.014	0.024	1.50	
HT-UTS AX8	Plate	0.074	0.12	2.05	bal	15.90	13.9	0.24	0.08	0.15	2.48	0.043	0.005	0.015	0.022		
HT-UTS CET1	Tubing	0.078	0.25	1.79	bal	16.85	14.3	0.21	0.10	0.52	2.26	0.039	0.006	0.025	0.011		
HT-UTS BWT4	Tubing	0.088	0.10	1.79	bal	15.04	13.7	0.10	0.17	0.44	2.19	0.016	0.004	0.002	0.008		
CRE 16-8-2 SS	Wire	0.062	0.74	2.12	bal	08.01	16.1	0.55			2.01	0.44	0.007	0.018	0.037		
ER17-14CuMo	Electrode	0.150	0.23	2.20	bal	14.31	16.3	0.01	0.40	0.01	2.17	0.01		0.013	0.063	2.96	
ERNi3CR82	Wire	0.030	0.18	3.05	2.30	bal	20.0	0.45	2.50			0.006		0.002		0.16	
alloy 556	Wire	0.130	0.38	0.97	bal	21.38	22.1		0.73		2.95	0.01		0.002	0.130		18Co; Zr; La

Table 2. Base metal/ Filler metal Combinations Tested in Creep

Alloy	Product	Condition	Filler Metal			
			alloy 82	17-14CuMo	CRE 16-8-2	alloy 556
316SS	Plate	mill			T,L	
316SS	Tubing	mill			T	
CRE 16-8-2	Weld deposit	as-welded			L	
17-14CuMo SS	Forging	mill		T		
17-14CuMo SS	Weld deposit	aged		L		
HT-UTS CE1	Plate	hot rolled		T		
HT-UTS CE2	Plate	hot rolled	T			
HT-UTS CE3	Plate	hot rolled				T
HT-UTS AX5	Plate	cold rolled		T		T
HT-UTS AX6	Plate	cold rolled		T	T	
HT-UTS AX7	Plate	cold rolled		T		T
HT-UTS AX8	Plate	cold rolled		T	L	
HT-UTS BWT4	Tubing	extruded			T	
HT-UTS BWT4	Tubing	5% cold sunk			T	
HT-UTS BWT4	Tubing	10% cold sunk			T	
HT-UTS BWT4	Tubing	12% cold sunk			T	T
HT-UTS BWT4	Tubing	creep tested			T	
HT-UTS BWT4	Tubing	Clad			T	
alloy 556	Plate	mill				T

T = Transverse L = Longitudinal

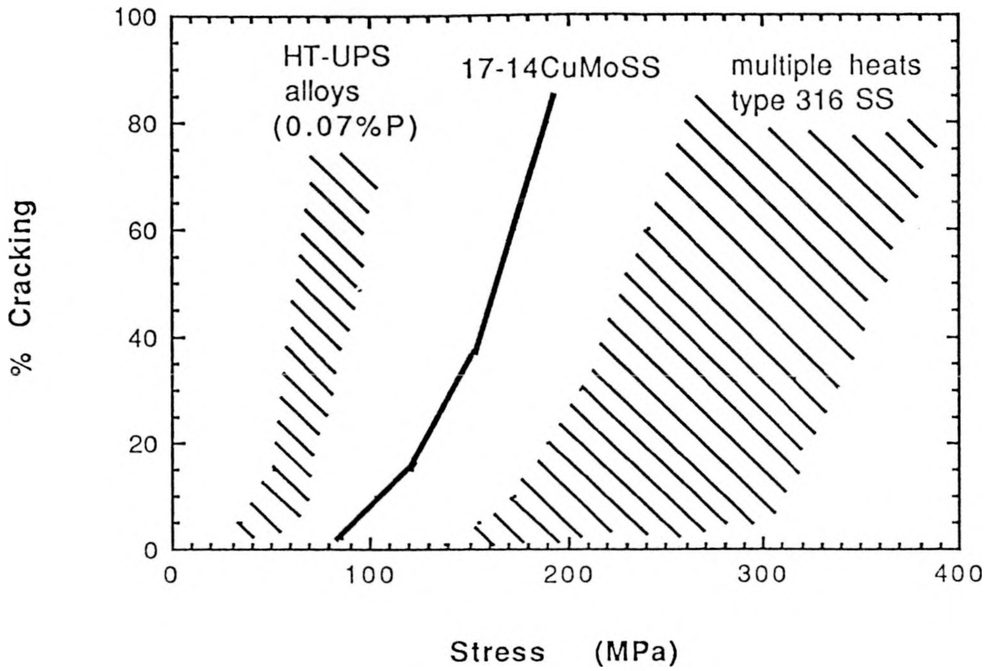

Figure 1. Comparison of the hot cracking tendencies of several base metals determined from Sigmajig testing.

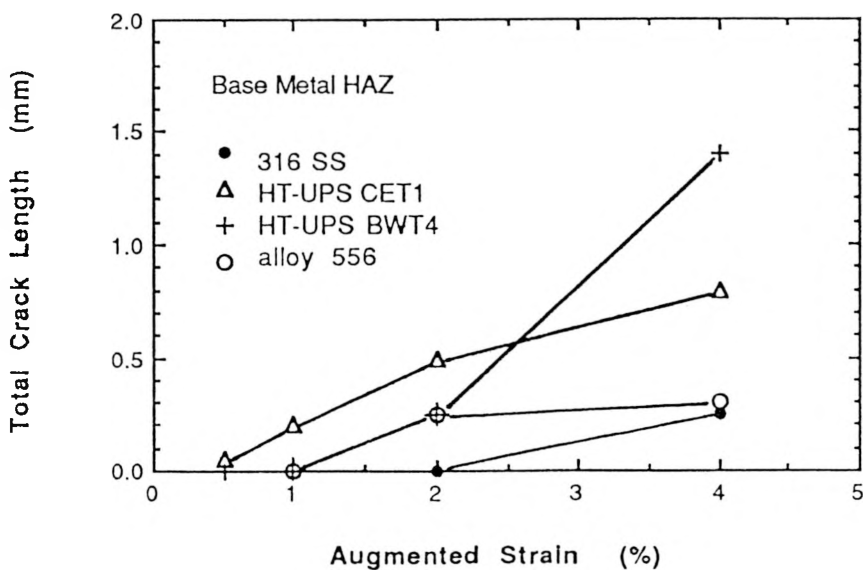

Figure 2. Comparison of the hot cracking tendencies of several base metals determined from Varestraint testing.

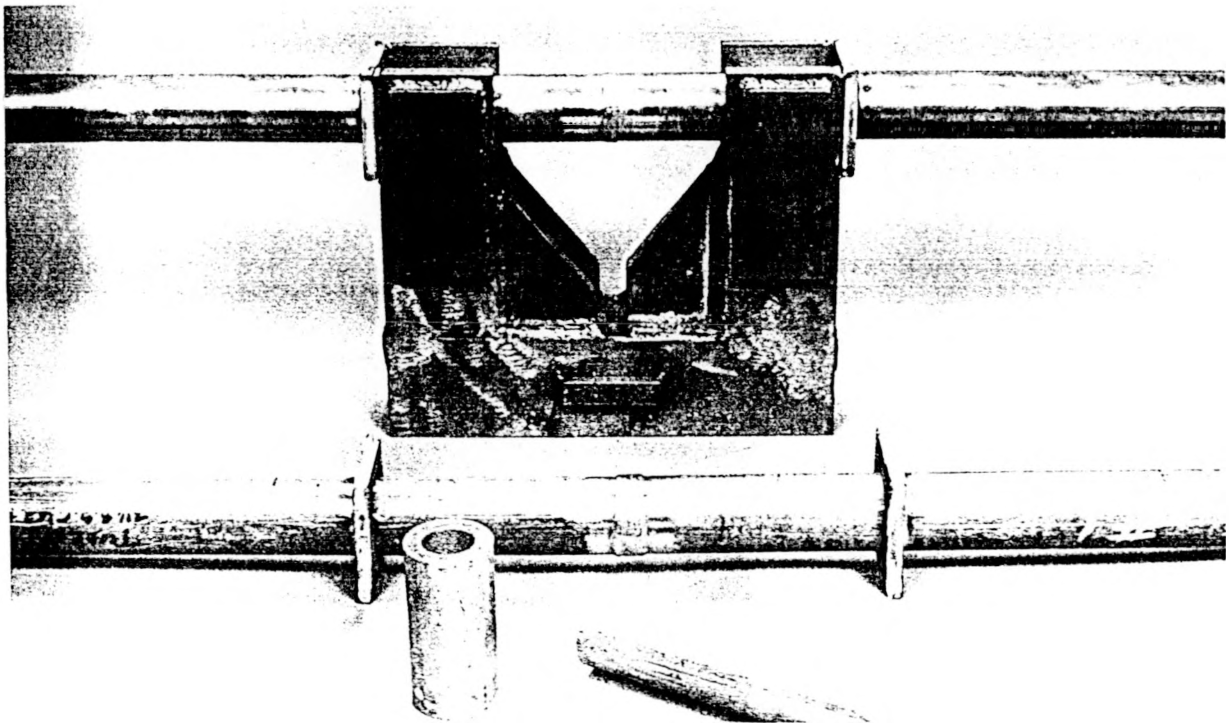

Figure 3. Fixture used for welding tubes under restraint.

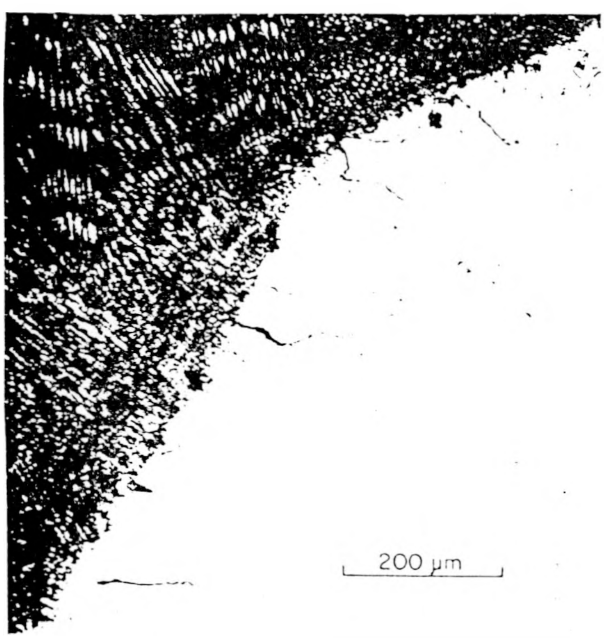

Figure 4. Typical HAZ cracks in high phosphorus (0.07%) HT-UPS alloys welded with ER 17-14CuMo stainless steel filler.

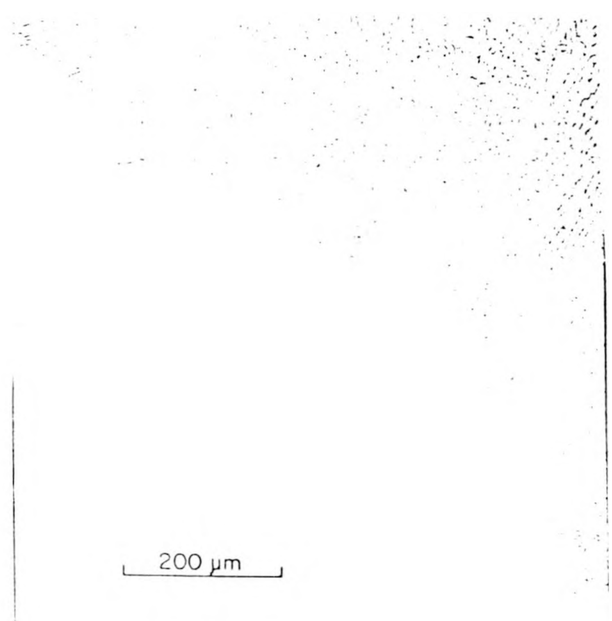

Figure 5. Sound weld in low phosphorus (0.016%) HT-UPS alloy BWT4 tube joined with CRE 16-8-2 stainless steel filler

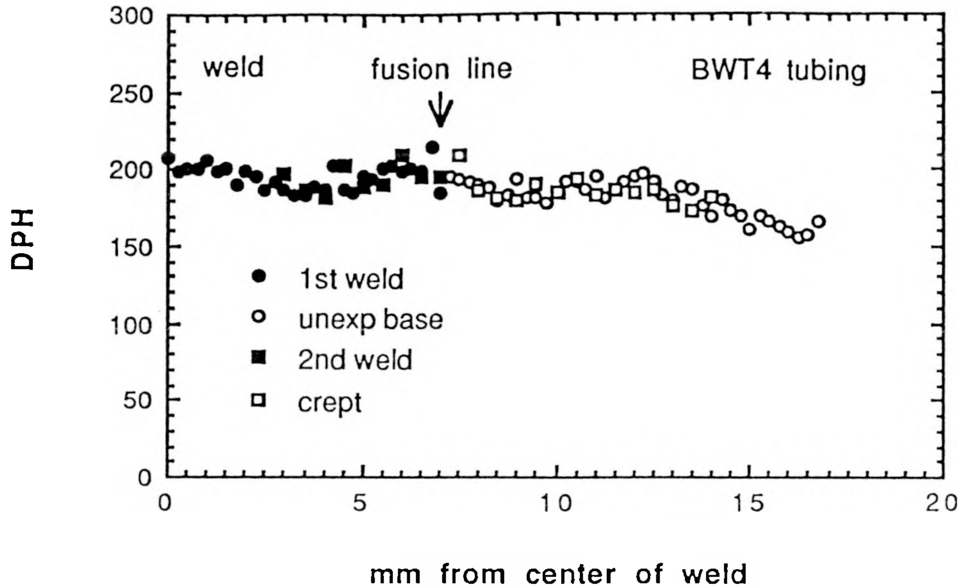

Figure 6. DPH hardness profile from the weld centerline through the HAZ of a HT-UPS alloy tube (BWT4/CRE 16-8-2) in both the as-extruded condition and after rewelding a tube exposed to creep at 700 °C for 2500 h.

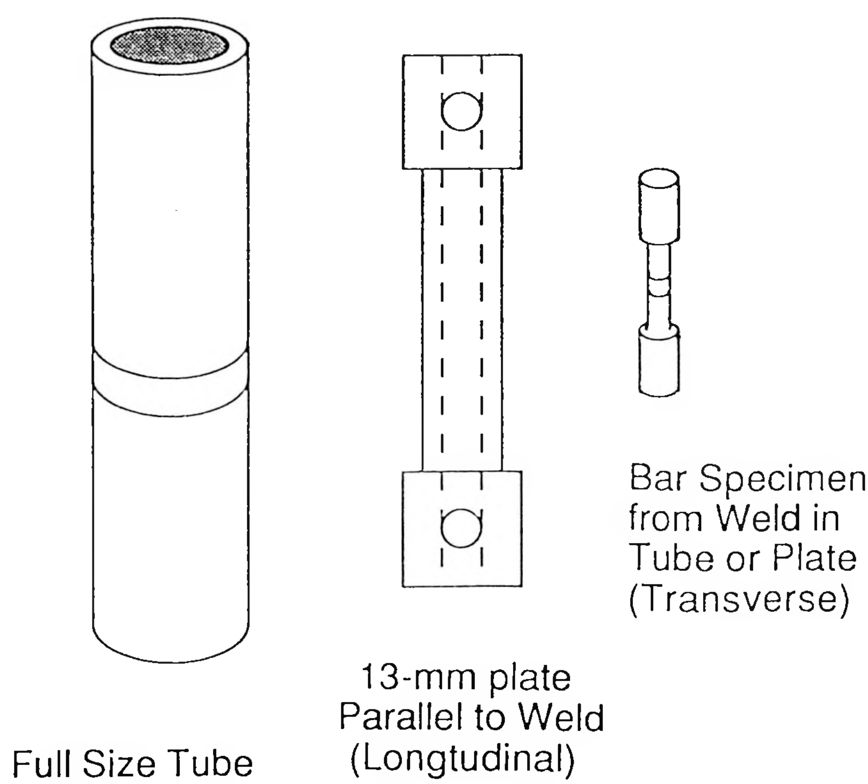

Figure 7. Specimens used for mechanical testing.

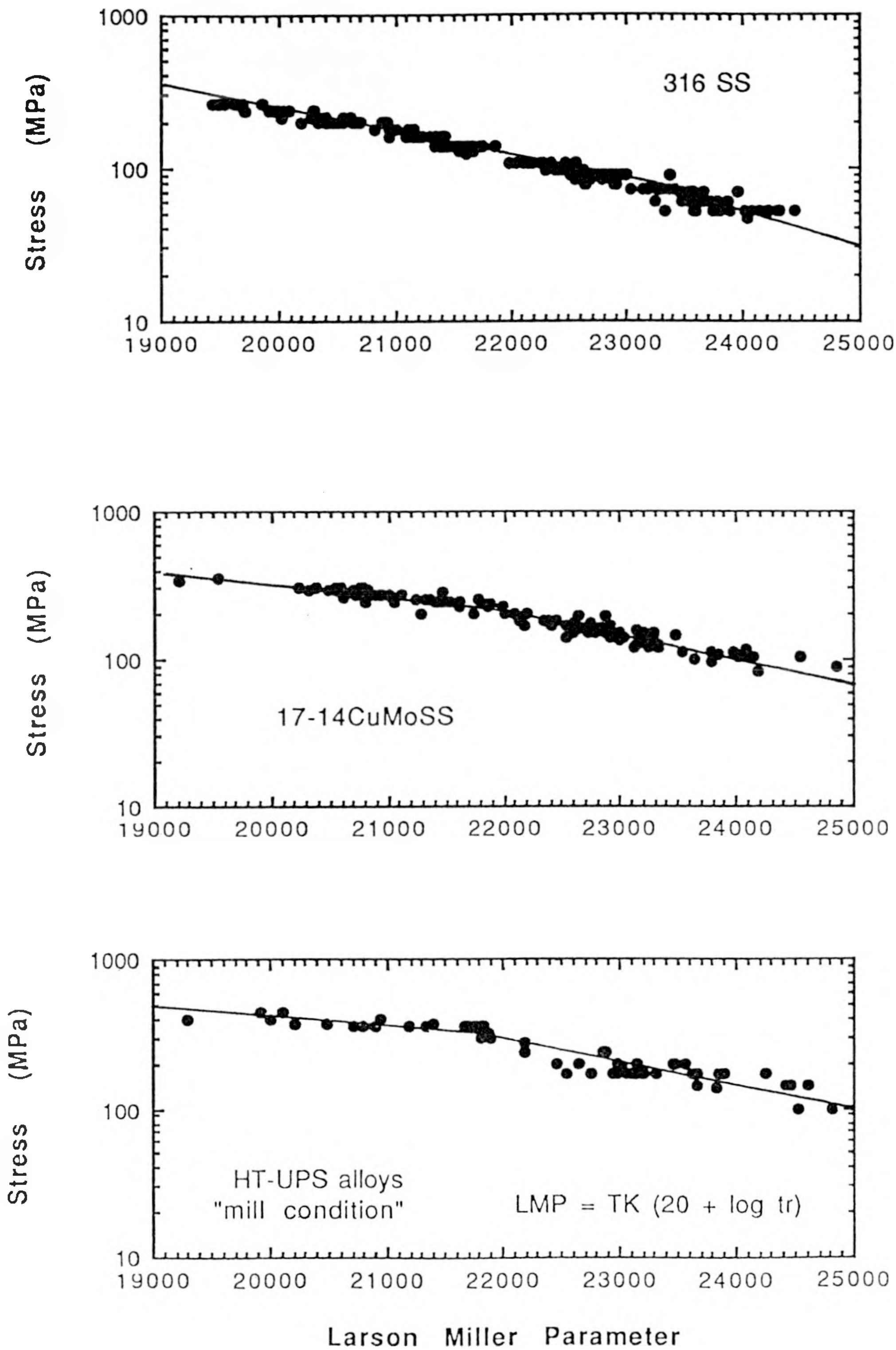

Figure 8. Log stress versus the Larson Miller parameter for the rupture life of three base metals: (a) type 316 stainless steel from NRIM; (b) type 17-14CuMo stainless steel; and (c) mill-annealed HT-UPS stainless steel.

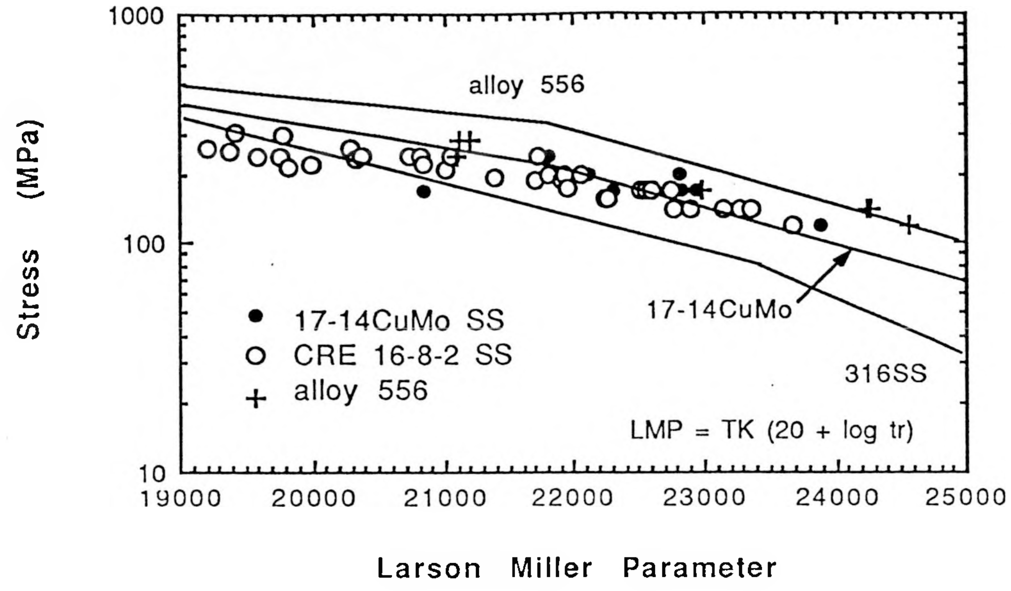

Figure 9. Comparison of the log stress versus LMP for the rupture life of weldments made from three filler metals with the trend curves for three base metals.

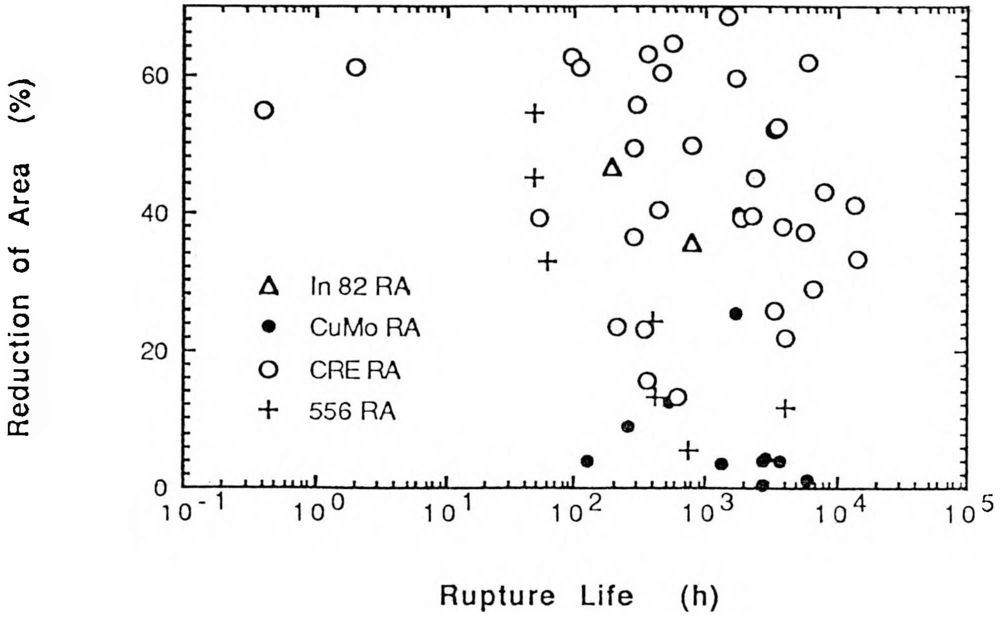

Figure 10. Reduction of area versus log time from rupture tests of weldments with four different filler metals.

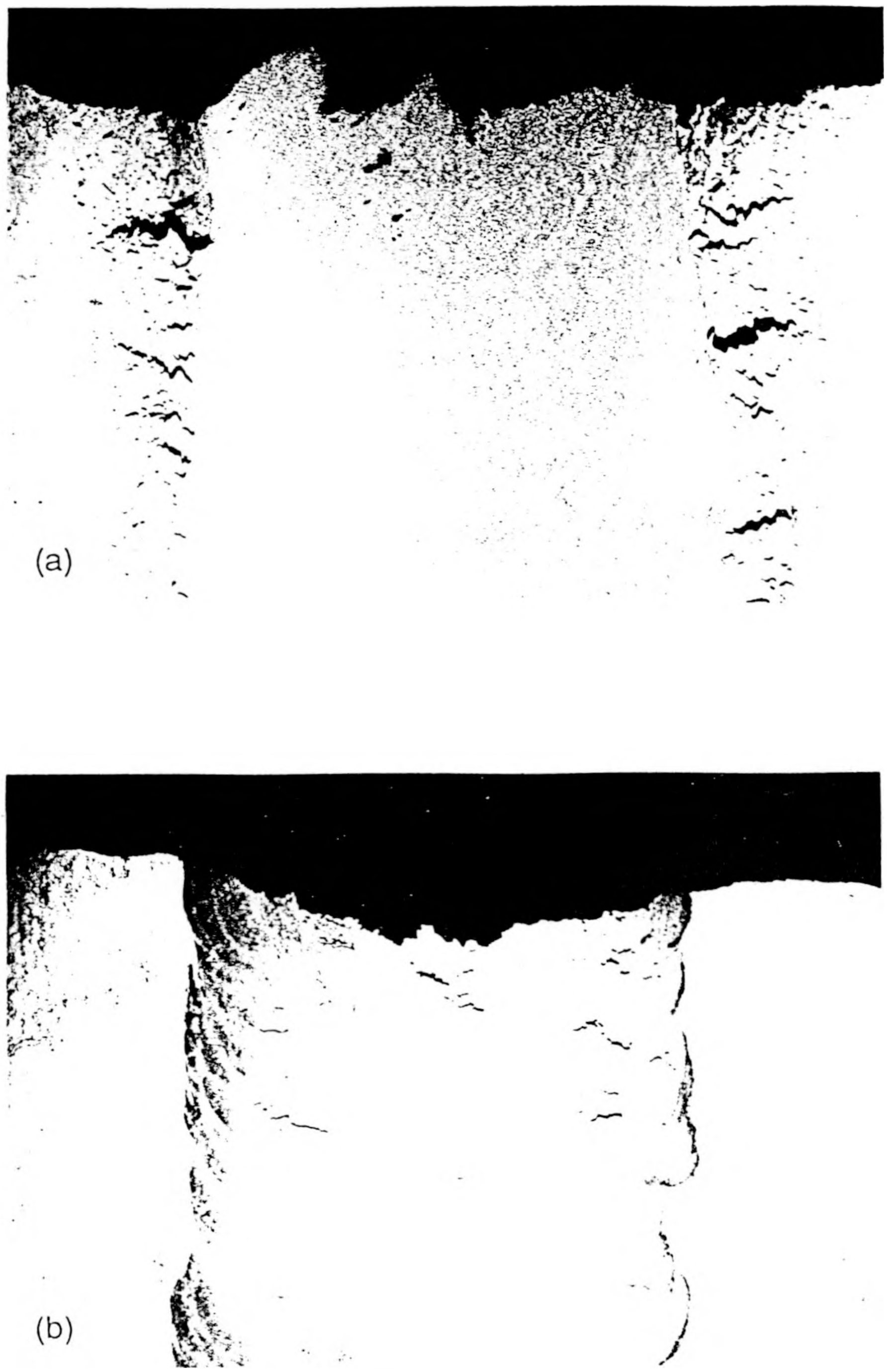

Figure 11. Cracking patterns in two longitudinally oriented weldment specimens creep tested at 650°C (a) type 316 stainless steel welded with CRE 16-8-2 filler metal that failed after 525 h at 170 MPa; (b) HT-UPS alloy (AX8) welded with CRE16-8-2 filler metal that survived 1000 h at 240 MPa, 1000 h at 290 MPa, and failed after 22 h at 340 MPa.